

ATP and Ca^{2+} (18). In skeletal muscle, αKAP , a non-kinase protein, has been identified as one of the anchoring proteins necessary for targeting the CaMKII holoenzyme to the SR membrane (19).

In single channel measurements, PKA-mediated phosphorylation of RyR decreased ATP and Mg^{2+} sensitivity, and the phosphorylated RyR channels exhibited an increase in the number of channel events and mean open time (20) and altered the Ca^{2+} sensitivity under non-steady-state conditions (21). In failing hearts, release of protein phosphatases from the RyR2 protein complex has been suggested to increase the endogenous PKA-mediated phosphorylation levels of RyR2 ("hyperphosphorylation") (9). Recently hyperphosphorylation and FKBP12 depletion of the skeletal ryanodine receptor during heart disease have been described and linked to the severely decreased exercise capability observed in these patients (22). Failing to observe dissociation of protein phosphatase 1, the only phosphatase known to associate with RyR1, during heart failure indicates a novel mechanism for PKA-mediated hyperphosphorylation of RyR1 in skeletal muscle (23). In both RyR1 and RyR2, hyperphosphorylation of the receptor was accompanied by an almost complete elimination of FKBP12 and FKBP12.6 binding to the receptor (9, 23). Loss of FKBP was proposed to increase RyR sensitivity to the agonist Ca^{2+} and thereby increase SR Ca^{2+} "leakiness" at diastolic Ca^{2+} levels (9, 23, 24). Other studies failed to establish a role for PKA-mediated phosphorylation on RyR activity (25, 26).

To investigate the functional effects of RyR phosphorylation in more detail, we prepared recombinant RyR1 and RyR2 phosphorylation mutants that cannot be phosphorylated at their known phosphorylation site, RyR1-Ser-2843 and RyR2-Ser-2809, due to an alanine or aspartic acid substitution. These amino acid substitutions mimic a constitutively dephosphorylated and phosphorylated receptor state, respectively. Functional and biochemical effects of these mutations were assessed using [^3H]ryanodine binding, single channel, and calcium imaging measurements as well as co-immunoprecipitation. The results presented here suggest that ryanodine receptors may be phosphorylated at additional site(s) *in vivo* and that phosphorylation of RyR1-Ser-2843 and RyR2-Ser-2809, *per se*, does not cause major functional changes.

EXPERIMENTAL PROCEDURES

Materials—Phospholipids were obtained from Avanti Polar Lipids (Birmingham, AL). [^3H]Ryanodine and [^{32}P]PO $_4^{3-}$ were purchased from PerkinElmer Life Sciences and ICN Biomedicals Inc. (Costa Mesa, CA), respectively. FK506 was generously provided by Dr. Bekershy, Fujisawa Healthcare Inc., Deerfield, IL. All chemicals used were of analytical grade.

Site-directed Mutagenesis and Cell Culture—The full-length rabbit RyR1 cDNA was constructed as described previously (27). Full-length rabbit RyR2 was kindly provided by Dr. Junichi Nakai, National Institute of Physiological Science, Okazaki, Japan. cDNAs encoding RyR1-S2843A and -S2843D and RyR2-S2809A and -S2809D mutants were prepared using *Pfu* polymerase-based chain reaction and the QuikChange site-directed mutagenesis kit according to the manufacturer's instructions (Stratagene, La Jolla, CA). The sequences of the primers used for mutagenesis were as follows: RyR1-S2843A, g aca cgg aag att Gcc cag act gcc cag; RyR1-S2843D, g aaa aag aca cgg aag att GAc cag act gcc cag acc tac; RyR2-S2809A, ga act cgt cgt att Gct cag aca agc cag g; RyR2-S2809D, cc ctt tat aac cga act cgt cgt att GAt cag aca agc c. The PvuI/NdeI (positions 8600–11304) fragment of RyR1 cDNA and the MunI/XbaI (positions 7736–10066) fragment of RyR2 subcloned into vector served as the template for mutagenesis. The complete mutated sequences were confirmed by DNA sequencing. The RyR1 mutated sequence was subcloned back into the original position of RyR1 in two steps: to a vector containing PvuI/XbaI (positions 8600–15276) fragment and preparation of mutated RyR1 full-length plasmids by ligation of two fragments (ClaI/PvuI and PvuI/XbaI containing the mutated sequence) and pCMV5 (ClaI/XbaI). The RyR2 fragment with the muta-

tion was subcloned back into the original position of RyR2 in two steps: to a vector containing BbrPI/SacII (positions 5038–11203) fragment and to full-length RyR2 in pCIneo. Nucleotide numbering is as described previously (27, 28).

WT and mutant RyRs were transiently expressed, in the presence of FKBP12.6 where indicated, in HEK293 cells using FuGENE 6 (Roche Applied Science) according to the manufacturer's instructions. Cells were maintained at 37 °C and 5% CO $_2$ in high glucose Dulbecco's modified Eagle's medium containing 10% fetal bovine serum and plated the day before transfection. For each 10-cm culture dish, 3.5 μg of cDNA was used. Cells were harvested 48 h after transfection. Crude membrane fractions were prepared as described previously (27) and stored under liquid nitrogen until use.

Preparation of SR Vesicles—SR vesicle fractions enriched in [^3H]ryanodine binding were prepared from rabbit skeletal and canine cardiac muscle in the presence of protease inhibitors (100 nM aprotinin, 1 μM leupeptin, 1 μM pepstatin, 1 mM benzamidine, 0.2 mM phenylmethylsulfonyl fluoride) (29, 30).

Single Channel Measurements—Single channel measurements were performed in symmetric KCl solutions (250 mM, 20 mM KHepes, pH 7.4) containing additions as indicated (31). Membrane fractions containing the WT and mutant receptors were added to the *cis* chamber of a bilayer apparatus and fused in the presence of an osmotic gradient with Mueller-Rudin type planar bilayers containing a 5:3:2 mixture of bovine brain phosphatidylethanolamine, phosphatidylserine, and phosphatidylcholine (35 mg of total phospholipid/ml *n*-decane). The gradient was formed across the bilayer membrane with 250 mM *cis* KCl and 20 mM *trans* KCl solutions. After appearance of single channel activity, an increase in *trans* KCl concentration to 250 mM prevented further incorporation of RyRs. The *trans* side of the bilayer was defined as ground. Channel activities were recorded at -20 mV and with 10 mM Ca^{2+} in the *trans* chamber at 0-mV holding potential using a commercially available patch clamp amplifier with a bilayer headstage (Axopatch 1D, Axon Instruments, Burlingame, CA). Measurement of the sensitivity of the channels to cytosolic Ca^{2+} indicated that in a majority of recordings (>98%) the cytosolic side of RyRs faced the *cis* side and the luminal side faced the *trans* side of the bilayer. Electrical signals were filtered at 2 kHz or 300 Hz with K $^+$ and Ca^{2+} as current carrier, respectively, and digitized at 10 kHz. Data acquisition and analysis were performed with the software package pClamp 9.0.2. (Axon Instruments, Union City, CA). Data files were directly acquired using the continuous gap-free mode. Channel parameters were calculated from current recordings of 2-min duration using a threshold setting of 50% of the current amplitude between the closed and open states. Channel open probability (P_o) in multichannel recordings was calculated using the formula $\sum i P_{o,i} / N$ where N is the total number of channels, and $P_{o,i}$ is channel open probability of the i th channel. The presence of possible substates relative to the full-open amplitude was probed using current amplitude histograms obtained from 2-min single channel recordings.

[^3H]Ryanodine Binding—Ryanodine binds with high specificity to the RyRs and is widely used as a probe of channel activity because of its preferential binding to the open channel state (4, 32). Unless otherwise indicated, experiments were performed as described previously (33). Membrane fractions (25–75 μg of protein in 120 μl of total sample volume) were incubated with 2.5 nM [^3H]ryanodine in 10 mM imidazole, pH 7.0 buffer containing 150 mM KCl, 0.3 M sucrose, under oxidizing (1 mM oxidized glutathione, GSSG) or reducing (5 mM reduced glutathione, GSH) conditions, and the indicated additions of channel agonists and/or antagonists. After 24 h at room temperature, samples were diluted with 8.5 volumes of ice-cold water and placed on Whatman GF/B filters preincubated with 2% polyethylenimine in water. Radioactivity remaining on the filters was determined by liquid scintillation counting to obtain bound [^3H]ryanodine. Nonspecific binding was determined using a 1000-fold excess of unlabeled ryanodine in the presence of 1 mM EGTA. The total number of ryanodine binding sites (B_{max}) was determined in 10 mM imidazole, pH 7.0 buffer containing 800 mM KCl, 200 μM free Ca^{2+} by Scatchard plot analysis or at 30 nM [^3H]ryanodine, a condition that caused maximal binding of [^3H]ryanodine to the receptors. If not stated differently, data were normalized using B_{max} values.

In experiments using protein phosphatase-treated SR, acid phosphatase (Sigma) was dialyzed for 5 h at 4 °C against sample buffer, and membranes were subsequently incubated with phosphatase at 60 μg of protein/unit of protein phosphatase for 1 h at 37 °C. RyR2-Ser-2809 phosphorylation levels of treated and untreated samples were determined by immunoblot analysis using a phospho-RyR2-Ser-2809- and dephospho-RyR2-Ser-2809-specific antibody (Badrilla, Leeds, UK). Development and analysis of Western blots were performed as described under "Co-immunoprecipitation of RyRs and FKBP" except that 5%

bovine serum albumin in Tris-buffered saline was used for blocking and primary antibody incubation medium, and Tris-buffered saline with 0.05% Tween 20 was used as washing buffer.

Co-immunoprecipitation of RyRs and FKBP—For immunoprecipitation experiments, membranes (1–2 mg of protein) were homogenized in ice-cold 20 mM NaPipes, pH 7.2 buffer containing 0.3 M sucrose, 1 M NaCl, 2.5% Triton X-100, and protease inhibitors (Complete choice protease inhibitor tablets, Roche Applied Science) using a Teflon homogenizer. Following a 10-min incubation on ice, samples were diluted with ice-cold water to 1.25% Triton X-100 and incubated on ice for an additional 20 min. Solubilized receptors were separated by centrifugation at 100,000 $\times g$ for 40 min, diluted with 20 mM NaPipes, pH 7.0 buffer containing 0.3 M sucrose, 5 mM dithiothreitol, 1.2 mM CaCl₂, and protease inhibitors to 0.3% Triton X-100 and 125 mM NaCl, and incubated with mouse monoclonal antibody RyRD110 (1:10) raised against rabbit skeletal muscle RyR and mouse monoclonal antibody RyRC3-33 (1:10) raised against cardiac muscle RyR at 4 °C. After 12 h, anti-mouse IgG-agarose beads (Sigma) were added, and the sample was incubated for an additional 2 h. Subsequently beads were washed three times with 20 mM NaPipes, pH 7.0 buffer containing 0.3% Triton X-100 and 125 mM NaCl and once with phosphate-buffered saline (PBS) to remove residual Triton X-100. Bound proteins were solubilized in SDS buffer at 37 °C for 15 min and separated on 3–15% gradient SDS-polyacrylamide gels. Proteins in the top half of the gel (>60 kDa) were transferred in a cooled wet chamber for 1 h at 400 mA and 12 h at 1000 mA onto a polyvinylidene difluoride membrane (Millipore) and blocked with 5% milk and 0.05% Tween 20 in PBS. RyRs were detected using monoclonal antibody RyRD110 and monoclonal antibody RyRC3-33, both diluted to 1:10 with 5% milk and 0.05% Tween 20 in PBS. The bottom half of the gel was transferred in a semidry chamber overnight at 50 mA onto polyvinylidene difluoride, blocked with 5% milk and 0.05% Tween 20 in PBS, and blotted with anti-FKBP antibody (Alexis) diluted to 1:2000 in 5% milk and 0.05% Tween 20 in PBS. RyR and co-immunoprecipitated FKBP were detected using enhanced chemiluminescence (ECL) (Amersham Biosciences), and proteins were quantified using Kodak Scientific Imaging Systems 1D version 3.6 software.

Calcium Imaging—Cellular Ca²⁺ release in response to caffeine was determined by intracellular fluo-4 fluorescence. HEK293 cells transfected with cDNA encoding WT and mutant RyRs were grown on glass coverslips. RyR2 cDNAs were co-transfected with FKBP12.6 cDNA. For control experiments, non-transfected cells or cells transfected with vector-only plasmids were used. Calcium imaging experiments were performed similarly to those described in Ref. 34. Approximately half-confluent cells were loaded with 5 μ M fluo-4 ester, 0.1% dispersion agent (F-127) at 37 °C in Krebs-Ringer-Henseleit solution (KRH) containing 125 mM NaCl, 5 mM KCl, 1.2 mM KH₂PO₄, 6 mM glucose, 1.2 mM MgCl₂, 2 mM CaCl₂, and 25 mM Hepes, pH 7.4. After 1 h, cells were rinsed with KRH to remove non-hydrolyzed fluorophore and transferred to a chamber. The fluorescence response was measured using a Nikon Eclipse TE300 microscope and Photon Technology International Deltascan system. Fluo-4 was excited at 490 nm, and emitted fluorescence was recorded at 526 nm. Base-line fluorescence was adjusted to 30–40 response units and recorded for 30 s, and caffeine responsiveness of cells was measured by rapid (~1-s) addition of freshly made caffeine solution to a final concentration of 10 mM. Preliminary experiments indicated that this concentration was sufficient to result in maximal caffeine response. To allow normalization, cells were subsequently treated with ionomycin to measure fluorescence in the presence of 2 mM Ca²⁺. For analysis, individual cells were defined as regions of interest, and average fluorescence was quantified using the program ImageMaster (Photon Technology International). Background levels were subtracted, and responsiveness was normalized using the analysis program Felix (Photon Technology International).

Metabolic Labeling of RyR2—In metabolic labeling experiments, ~2–3 $\times 10^7$ HEK293 cells were used. To increase the extent of metabolic ³²P_i labeling, cells were incubated for 1 h in phosphate-free Dulbecco's modified Eagle's medium prior to labeling for 12 h in fresh phosphate-free medium supplemented with 100 μ Ci/ml ³²P_i (ICN Biomedicals Inc.). PBS and all other buffers used for harvesting and processing the cells contained Complete choice protease inhibitor tablets (Roche Applied Science) and phosphatase inhibitor mixture I (Sigma), 1 mM Na₃VO₄, and 75 mM Na₃PO₄. Crude membrane fractions from metabolically labeled HEK293 cells were solubilized in 20 mM NaPipes, pH 7.4 buffer containing 0.3 M sucrose, 2.5% Triton X-100, and 1 M NaCl. Extended solubilization times of 4 h were required before affinity purification to eliminate a ³²P-labeled high molecular weight band traveling closely above the RyR on the gels. Following dilution to 0.3% Triton X-100 and 125 mM NaCl, RyR2 was purified by binding to

CaM-agarose beads in the presence of 900 μ M free Ca²⁺ and 3 mM dithiothreitol. Following washing of the beads, proteins were separated by 3–10% SDS-PAGE. Gels were silver-stained and dried using a gel drying solution (Invitrogen), and the incorporation of ³²P_i was visualized using phosphorimaging (Storm PhosphorImager, ImageQuant analysis software, and general purpose screens, all obtained from Amersham Biosciences). In parallel experiments, unlabeled cells were processed identically. The position of RyR2 as determined by Western blot analysis was used to identify the silver-stained RyR2 bands in the ³²P_i-labeled gels and PhosphorImager scans. To quantify the amount of ³²P_i incorporation, identically sized gel pieces containing the RyR2 band were incubated with scintillation fluid for 24 h and counted using a scintillation counter. To account for potential differences in initial ³²P_i uptake by the cells, ³²P content of a second gel piece at 200-kDa molecular mass was determined and used to normalize the RyR2 signal. Background signal intensities of non- and vector-only-transfected cells were determined and subtracted from all samples, and final results were adjusted for RyR2 protein content based on signal intensity in silver-stained gels and Western blots. Western blot and silver stain gave consistent data regarding the RyR2 protein content.

Determination of Free Ca²⁺ Concentrations—Different free Ca²⁺ concentrations were prepared by mixing CaCl₂ and EGTA as determined using the stability constants and computer program published previously (35). Free Ca²⁺ concentrations of ≥ 1 μ M were verified with the use of a Ca²⁺-selective electrode (detectION, Philadelphia, PA), and those of <1 μ M were determined using fluo-3.

Data Analysis—Results are given as means \pm S.E. with the number of experiments in parentheses. Significance of differences in the data ($p < 0.05$) was determined using Student's *t* test.

RESULTS

We used site-directed mutagenesis to prepare skeletal and cardiac RyR mutants that carry an alanine or aspartic acid substitution at the conserved phosphorylation site, RyR1-Ser-2843 and RyR2-Ser-2809. To investigate channel characteristics in the absence of an endogenous receptor population, recombinant WT and mutant RyRs were transiently expressed in HEK293 cells. In this cell line, absence of an endogenous RyR pool was confirmed by (i) reverse transcriptase PCR in which no skeletal or cardiac RyR mRNAs were detected, (ii) lack of an RyR immunoblot signal in Western blots, and (iii) failure to observe a functional response in [³H]ryanodine binding and calcium imaging experiments (data not shown). Reverse transcriptase PCR experiments indicated that both FKBP12 and -12.6 mRNA were present in HEK293 cells with FKBP12 mRNA being more abundant. Similarly we found that in immunoblots the expression level of FKBP12 exceeded that of FKBP12.6 (data not shown).

RyR expression levels were determined by Scatchard plot analysis. Transfection using RyR1 cDNA resulted in expression levels of 0.1–0.2 pmol/mg of protein as determined by [³H]ryanodine binding; cardiac RyR expression levels were 0.6–0.7 pmol/mg of protein. Scatchard plots of [³H]ryanodine binding to cardiac WT and mutant receptors showed similar B_{\max} values and no differences in K_d values ($n = 4$, mean $K_d \pm$ S.E.: WT-RyR2, 5.2 \pm 1.5 nM; RyR2-S2809A, 6.9 \pm 1.8 nM; RyR2-S2809D, 5.9 \pm 2.3 nM; data not shown).

RyR Phosphorylation Mutants Bind FKBP—Marks and colleagues (9, 23) have shown that PKA-mediated hyperphosphorylation of skeletal and cardiac RyRs is associated with the dissociation of the small FKBP. To determine whether the serine to alanine and aspartic acid mutants bound FKBP, we performed co-immunoprecipitation experiments. Recombinant WT and mutant RyR2s co-expressed with FKBP12.6 were solubilized in Triton X-100 as described under "Experimental Procedures," and the non-solubilized material was removed by centrifugation. RyR2s in the total and supernatant fractions were immunoprecipitated using anti-RyR2 antibody and analyzed by Western blots for RyR2 (Fig. 1A) and FKBP12.6 (Fig. 1B). Immunoprecipitates of the total and supernatant fractions yielded immunoreactive bands for both RyR2 and FKBP. The

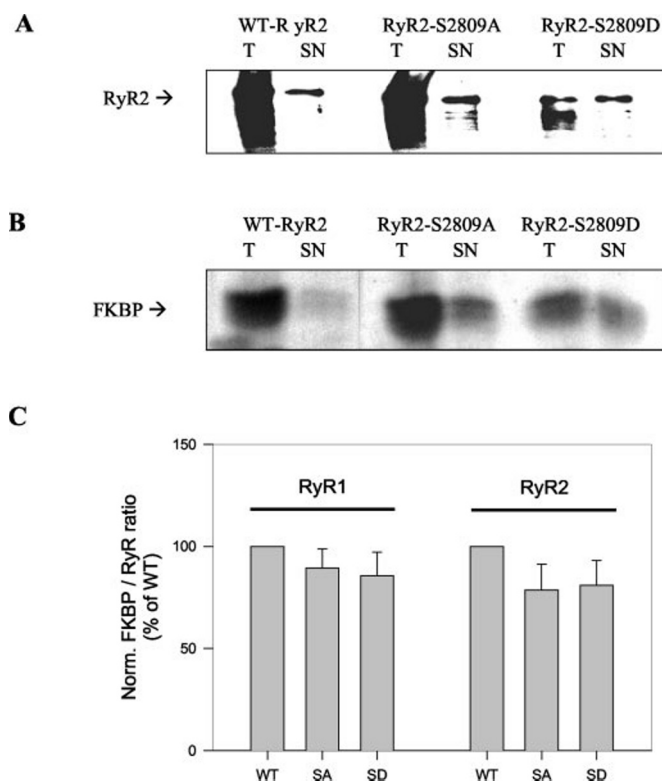


FIG. 1. Skeletal and cardiac RyR phosphorylation mutants bind FKBP. Membrane fractions containing recombinant WT and mutant channels were solubilized in 2.5% Triton X-100 and 1 M NaCl, and co-immunoprecipitation was performed using total (*T*, one-fifth the volume of supernatant) and supernatant (*SN*) fractions. *A*, immunoblot following immunoprecipitation of WT-RyR2 (*WT*), RyR2-S2809A (*SA*), and RyR2-S2809D (*SD*) from both total and supernatant fractions. *B*, immunoblot showing the pulled down FKBP from the same gel. *C*, pooled and normalized results from five co-immunoprecipitation experiments using supernatant fractions. Data are given as mean \pm S.E. No significant differences within the skeletal or cardiac groups were observed. *Norm.*, normalized.

total fractions (one-fifth the volume of supernatant samples) displayed higher signals than the supernatants, indicating that only a partial solubilization of the RyR-FKBP complexes had occurred. Fig. 1C summarizes results from five independent co-immunoprecipitation experiments using the supernatant fractions. The intensity of the RyR and FKBP bands and their ratio relative to WT-RyR1 and WT-RyR2 were determined. The skeletal and cardiac phosphorylation mutants showed no significant alterations in their FKBP/RyR binding ratio. In separate co-immunoprecipitation experiments using skeletal and cardiac SR vesicles and the recombinant WT-RyRs, similar relative FKBP/RyR ratios were obtained (data not shown). In control experiments, the use of agarose beads without addition of anti-RyR antibody or of non-transfected or vector-only-transfected cells or preincubation for 1 h at 37 °C with 10 μ M FK506 resulted in no detectable FKBP signals (not shown).

Mutation of the Phosphorylation Sites RyR1-Ser-2843 and RyR2-Ser-2809 Does Not Affect Channel Function—The functional properties of WT and mutant RyRs were determined in single channel measurements using the planar lipid bilayer method. Fig. 2A shows representative traces from WT-RyR1, RyR1-S2843A, and RyR1-S2843D. Channels were recorded in the presence of 2 μ M free Ca^{2+} on both sides of the bilayer at -20 -mV holding potential with K^+ as conducting ion (*top traces*). Under this condition, both the open probability (P_o) and gating of the mutant channels were indistinguishable from the WT receptor. The mutant and WT-RyR1 channels were also

recorded under more physiological conditions at 0-mV holding potential and using 10 mM luminal Ca^{2+} as conducting ion (*bottom traces*). In these recordings, the cytosolic free Ca^{2+} levels were lowered to 100 nM, and 1 mM ATP was added to the *cis* chamber. Again no significant differences were observed between WT and mutant receptors. Representative current histograms obtained from 2-min recordings of WT-RyR1 (*left*), RyR1-S2843A (*middle*), and RyR1-S2843D (*right*) with 10 mM Ca^{2+} as current carrier are shown in Fig. 2B. Histogram analysis indicated a main current amplitude of ~ 2.5 pA for WT and mutant channels. The occurrence of currents with lower amplitudes indicated the presence of subconductances or poorly resolved events. No significant differences in frequency or appearance of these events were observed between the WT and mutant RyR1 channels.

Fig. 3, *A* and *B*, shows the corresponding single channel recordings and current histograms for cardiac RyR channels that were co-expressed with FKBP12.6. The *left column* shows two representative WT current traces, and the *middle and right columns* show those for the RyR2-S2809A and RyR2-S2809D mutants, respectively. Channels were recorded with K^+ (*top traces*) at -20 -mV holding potential or with Ca^{2+} (*bottom traces*) as current carrier at 0-mV holding potential. Similar to RyR1, the current traces and current histograms of WT and the mutant channels did not show major differences. The paucity of currents with a lower amplitude than the main amplitude of ~ 2.5 pA indicated that subconductances were largely absent with 10 mM Ca^{2+} as current carrier.

The averaged open probability (P_o), number of events, and mean open (T_o) and close (T_c) times are shown in Table I for RyR1 and in Table II for RyR2. P_o values were determined using single and multiple channel recordings, whereas only single channel recordings were used for number of events, T_o , and T_c calculations. Some differences were observed between the kinetic parameters of the WT-RyRs and their corresponding phosphorylation mutants, but none of these were significant. The K^+ -conducting WT-RyR2, RyR2-S2809A, and RyR2-S2809D channels recorded at -20 -mV holding potential (top panel of Table II) were activated to a greater extent with 2 μ M Ca^{2+} on both sides of the bilayer, and the open times were more than 10-fold greater than those of the RyR1 channels (top panel of Table I). These isoform-dependent differences are a characteristic property of the two RyRs.

The functional properties of WT and mutant RyRs were also compared in [3H]ryanodine binding experiments. Fig. 4A shows the results of experiments investigating the regulation of skeletal WT and mutant RyRs by Ca^{2+} . Similar experiments were also performed with cardiac WT and mutant RyRs transiently co-expressed with FKBP12.6 in HEK293 cells (Fig. 4B). [3H]ryanodine binding resulted in similar, overlapping Ca^{2+} activation/ Ca^{2+} inactivation curves for WT-RyR1 and the two RyR1 mutants (Fig. 4A) and WT-RyR2 and the two RyR2 mutants (Fig. 4B). WT and mutant receptors showed a similar Ca^{2+} dependence under oxidizing (1 mM GSSG, Fig. 4, *A* and *B*) and reducing (5 mM GSH, not shown) conditions.

Phosphorylation of RyR by either PKA or CaMKII has been reported to attenuate Mg^{2+} inhibition of channel activity (15, 20, 36). We determined whether Mg^{2+} differentially inhibited the two RyR2 phosphorylation mutants. Recombinant WT and mutant RyR2s were incubated in a 0.15 M KCl buffer containing 1.4 mM Ca^{2+} and Mg^{2+} concentrations ranging from 0 to 10 mM. Increases in Mg^{2+} concentration resulted in a progressive decrease in [3H]ryanodine binding, however, without significant differences between WT and mutant RyR2s (Fig. 5A). Similarly 5 mM AMP-PCP, a non-hydrolyzable ATP analog, in the presence of 0.65 and 4 mM Ca^{2+} caused no significant

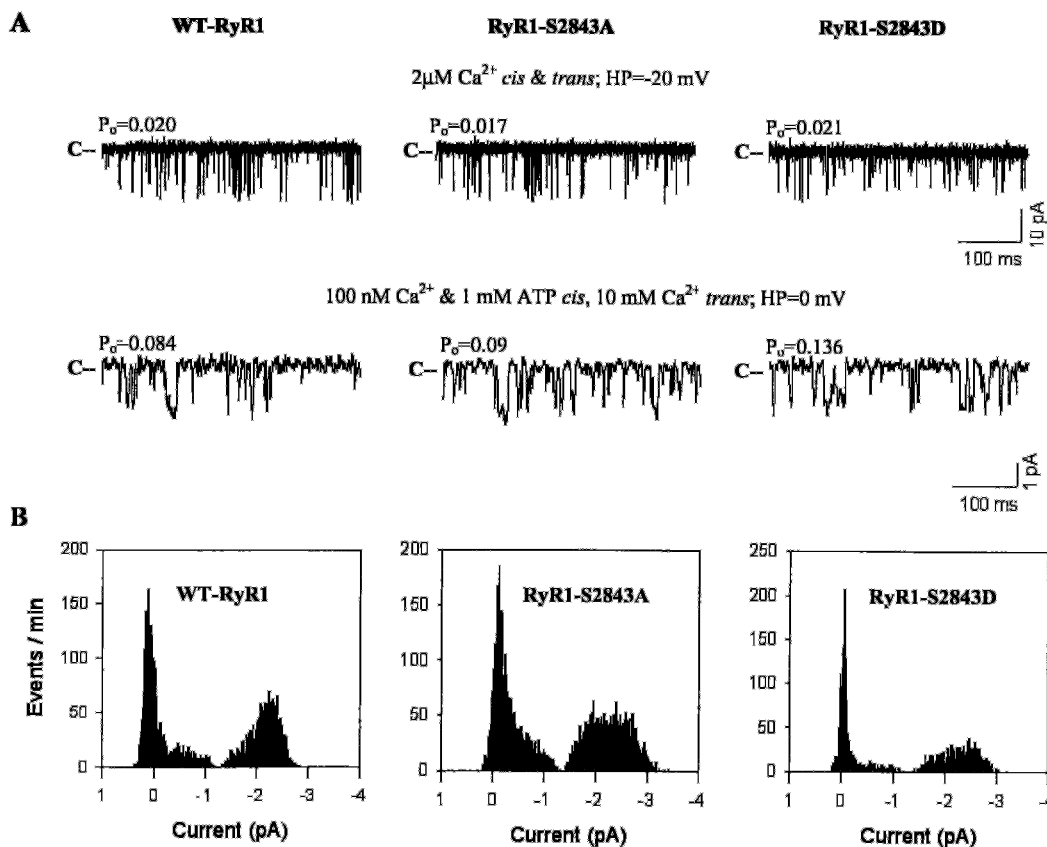


FIG. 2. **Single channel measurements of skeletal WT and mutant RyRs.** A, membrane fractions containing WT and mutant RyRs were added to the *cis* site of a lipid bilayer. Shown is one representative single channel recording for each of the following: WT-RyR1 (*left column*), RyR1-S2843A (*middle column*), and RyR1-S2843D (*right column*). Single channel currents shown as downward deflections from the closed levels (C-) were recorded at -20-mV holding potential in symmetrical 250 mM KCl, 20 mM KHepes, pH 7.4 in the presence of 2 μM free cytosolic Ca^{2+} (*top traces*). Channels were also recorded under more physiological, submaximal Ca^{2+} -activating conditions at 0 mV in symmetrical 250 mM KCl with 10 mM luminal Ca^{2+} in the presence of 1 mM cytosolic ATP and 100 nM cytosolic free Ca^{2+} (*bottom traces*). B, representative current histograms derived from 2-min recordings in the presence of 1 mM ATP and 100 nM free Ca^{2+} with 10 mM luminal Ca^{2+} as conducting ion.

changes in Mg^{2+} inhibition between mutant and WT receptors (Fig. 5B).

We also considered the possibility that the recombinant RyR channels with a serine to aspartic acid substitution decreased the Ca^{2+} content of HEK293 cells by forming "leaky" Ca^{2+} channels (9, 23). In Fig. 6, intracellular Ca^{2+} release in response to a bolus of 10 mM caffeine was determined by intracellular fluo-4 fluorescence. The recordings in five representative, individual cells expressing WT-RyR1 are shown in Fig. 6A. Caffeine (10 mM) caused a rapid increase in free Ca^{2+} as indicated by the 2–3-fold rise in fluo-4 fluorescence from base-line levels that abated in ~ 60 s. Peak caffeine responses were normalized by permeabilizing the cells to Ca^{2+} (2 mM) present in KRH. Addition of the Ca^{2+} ionophore ionomycin increased the fluorescence intensities proportional to those observed with caffeine. Only cells showing a >1.5 -fold increase in fluorescence in response to caffeine addition (typically 40–50%) were included in the analysis. Fig. 6B summarizes the results from at least two separate cell preparations and combines data from 15–27 cells expressing skeletal WT and mutant RyRs and 22–44 cells expressing cardiac WT and mutant RyRs. For both isoforms, no significant differences in the size of the caffeine-sensitive Ca^{2+} stores were observed between WT and mutants.

Dephosphorylation of Ser-2809 Does Not Affect Calcium Response of Canine SR—Dephospho-Ser-2809 and phospho-Ser-2809 antibodies were used to determine the level of RyR2-Ser-2809 phosphorylation in cardiac SR membranes. Fig. 7 (*inset*) shows a strong RyR2-immunoreactive band using the phospho-

Ser-2809 antibody. A weak signal was detected using the dephospho-Ser-2809 antibody. Acid phosphatase treatment almost completely abolished phospho-Ser-2809 immunoreactivity while causing an ~ 4 -fold increase in the dephospho-Ser-2809 signal. The functional consequences of Ser-2809 dephosphorylation were examined in [^3H]ryanodine binding measurements. Fig. 7 shows essentially identical Ca^{2+} activation/ Ca^{2+} inactivation binding curves for cardiac SR membranes that were treated and not treated with acid phosphatase. Alkaline phosphatase treatment also was without significant effect on Ca^{2+} dependence of treated SR (data not shown).

Evidence for Additional Phosphorylation Sites in RyR2—We also explored the possibility that additional sites in RyR are phosphorylated. Mutant and WT cardiac receptors were expressed in the presence of $^{32}\text{P}_i$ and isolated using a CaM-agarose batch purification protocol. Proteins retained on the beads were separated by 3–10% SDS-PAGE. Western blots of unlabeled samples showed that solubilized native and recombinant RyR2s bind to the CaM-agarose beads (Fig. 8A). Addition of 3 μM CaM abolished binding, thereby confirming the specificity of the CaM and RyR interaction. Fig. 8B shows the silver-stained gels of metabolically labeled WT-RyR2, RyR2-S2809A, and RyR2-S2809D. RyR2s were bound in the presence and absence of 3 μM CaM to correct for nonspecific binding. The corresponding autoradiogram is shown in Fig. 8C; WT and mutant RyR2s all incorporated $^{32}\text{P}_i$ radioactivity. The amount of radioactivity in the RyR band was measured in a scintillation counter, normalized for the RyR2 content as determined by

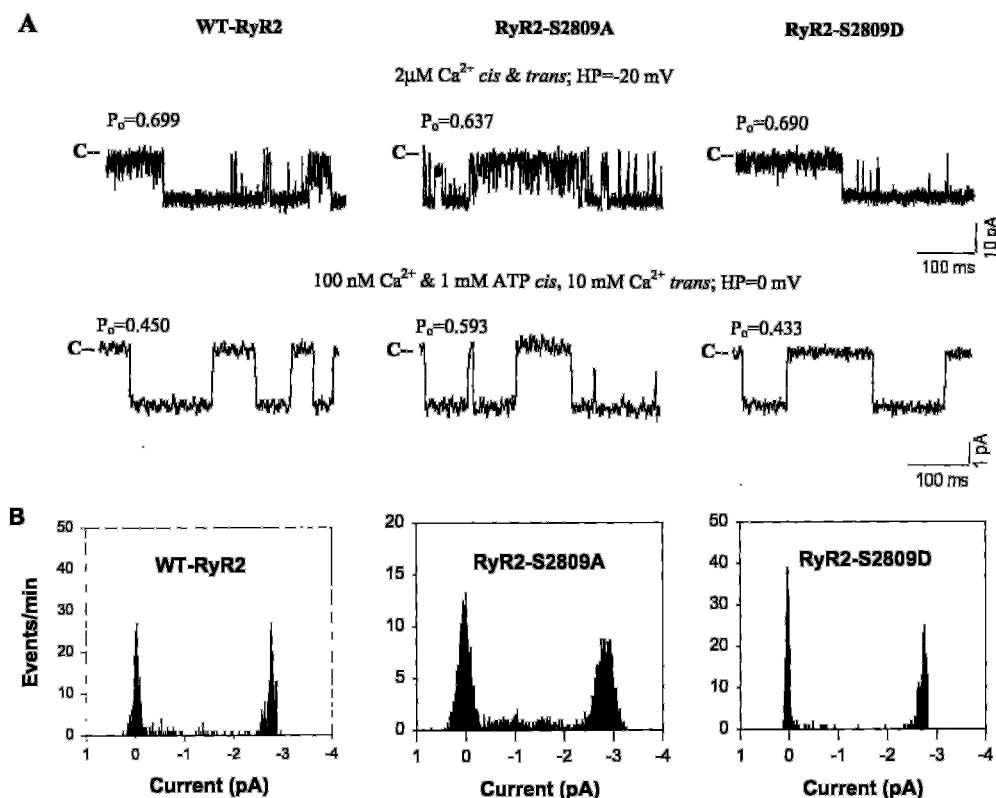


FIG. 3. **Single channel measurements of cardiac WT and mutant RyRs.** *A*, membrane fractions containing WT-RyR2, RyR2-S2809A, and RyR2-S2809D and co-expressed FKBP12.6 were added to the *cis* site of a lipid bilayer. Shown is one representative single channel recording for each of the following: WT-RyR2 (*left column*), RyR2-S2809A (*middle column*), and RyR2-S2809D (*right column*). Single channel currents shown as downward deflections from the closed levels (C-) were recorded as in Fig. 2. *B*, representative current histograms derived from 2-min recordings in the presence of 1 mM ATP and 100 nM free Ca^{2+} with 10 mM luminal Ca^{2+} as conducting ion.

TABLE I

Steady-state and kinetic single channel parameters for skeletal wild type RyR and phosphorylation mutants

Channel open probability (P_o) was determined from single and multiple channel recordings of 2-min duration. Number of events and mean open (T_o) and mean close (T_c) times were calculated from 2-min recordings of single channel activities. Results are given as the mean \pm S.E. with the number of experiments in parentheses. HP, holding potential.

	P_o	Events/min	T_o	T_c
			ms	ms
2 $\mu\text{M Ca}^{2+}$ cis and trans, HP = -20 mV				
WT-RyR1	0.029 \pm 0.007 (10)	5,482 \pm 2,068 (5)	0.41 \pm 0.03 (5)	55.52 \pm 25.08 (5)
RyR1-S2843A	0.156 \pm 0.075 (11)	10,399 \pm 3,508(4)	0.53 \pm 0.10 (4)	14.96 \pm 5.02 (4)
RyR1-S2843D	0.030 \pm 0.009 (9)	7,072 \pm 1,962(6)	0.40 \pm 0.05 (6)	22.53 \pm 4.73 (6)
0.1–0.3 $\mu\text{M Ca}^{2+}$ + 1 mM ATP cis, 10 mM Ca^{2+} trans, HP = 0 mV				
WT-RyR1	0.200 \pm 0.055 (10)	3,355 \pm 862 (5)	5.50 \pm 1.50 (5)	44.72 \pm 20.07 (5)
RyR1-S2843A	0.150 \pm 0.030 (11)	2,881 \pm 1,579(4)	3.20 \pm 0.59 (4)	120.11 \pm 64.51 (4)
RyR1-S2843D	0.121 \pm 0.030 (9)	2,760 \pm 560 (6)	4.30 \pm 0.62 (6)	48.93 \pm 16.14 (6)

the silver staining and Western blot signals, and corrected for ^{32}P background counts. The combined results from two independent experiments are shown in Fig. 8D. The finding of significant $^{32}\text{P}_i$ incorporation into the cardiac phosphorylation mutants suggests that RyR2 is phosphorylated at additional, so far uncharacterized phosphorylation sites. We note that in our experiments no attempt was made to activate CaMK or PKA, which could have altered the extent of phosphorylation of Ser-2809 relative to the additional sites.

DISCUSSION

Protein phosphorylation is a fundamental mechanism by which kinases and phosphatases regulate a wide variety of biological processes. In striated muscle, protein kinases and phosphatases modulate both contraction and relaxation by phosphorylating and dephosphorylating numerous SR proteins

that include the luminal Ca^{2+} -binding protein calsequestrin (37), the Ca^{2+} pump (38), its regulatory protein phospholamban (39), the RyR-associated proteins triadin (40, 41) and sorcin (42), and the Ca^{2+} release channel/ryanodine receptor (11). Changes in the phosphorylation levels are of interest due to the possibility that these contribute to an impaired SR and contractile function during heart failure. PKA and CaMKII phosphorylation of phospholamban results in an increased Ca^{2+} -ATPase activity (39). Perturbation of regulation of phospholamban phosphorylation by second messengers (39), along with other cellular changes, has been suggested as one possible mechanism leading to heart failure (25, 26). A second proposed mechanism is that PKA-mediated hyperphosphorylation of a conserved serine, Ser-2843 in the skeletal RyR and Ser-2809 in cardiac RyR, contributes to an impaired SR and aberrant con-

TABLE II

Steady-state and kinetic single channel parameters for cardiac wild type RyR and phosphorylation mutants

Channel open probability (P_o) was determined from single and multiple channel recordings of 2-min duration. Number of events and mean open (T_o) and mean close (T_c) times were calculated from 2-min recordings of single channel activities. Results are given as the mean \pm S.E. with the number of experiments in parentheses. HP, holding potential.

	P_o	Events/min	T_o	T_c
			ms	ms
2 μ M Ca^{2+} <i>cis</i> and <i>trans</i> , HP = -20 mV				
WT-RyR2	0.497 \pm 0.072 (10)	11,305 \pm 2,982(4)	7.86 \pm 3.91 (4)	6.29 \pm 2.51 (4)
RyR2-S2809A	0.359 \pm 0.060 (9)	11,247 \pm 3,714(5)	6.87 \pm 2.17 (5)	30.87 \pm 25.55 (5)
RyR2-S2809D	0.505 \pm 0.071 (10)	7,578 \pm 1,938(4)	10.08 \pm 3.85 (4)	8.69 \pm 4.11 (4)
0.1–0.3 μ M Ca^{2+} + 1 mM ATP <i>cis</i> , 10 mM Ca^{2+} <i>trans</i> , HP = 0 mV				
WT-RyR2	0.260 \pm 0.090 (8)	342 \pm 121 (4)	140 \pm 82 (4)	436 \pm 297 (4)
RyR2-S2809A	0.330 \pm 0.089 (9)	384 \pm 132 (5)	107 \pm 56 (5)	446 \pm 242 (5)
RyR2-S2809D	0.186 \pm 0.044 (10)	296 \pm 69 (4)	62 \pm 24 (4)	448 \pm 203 (4)

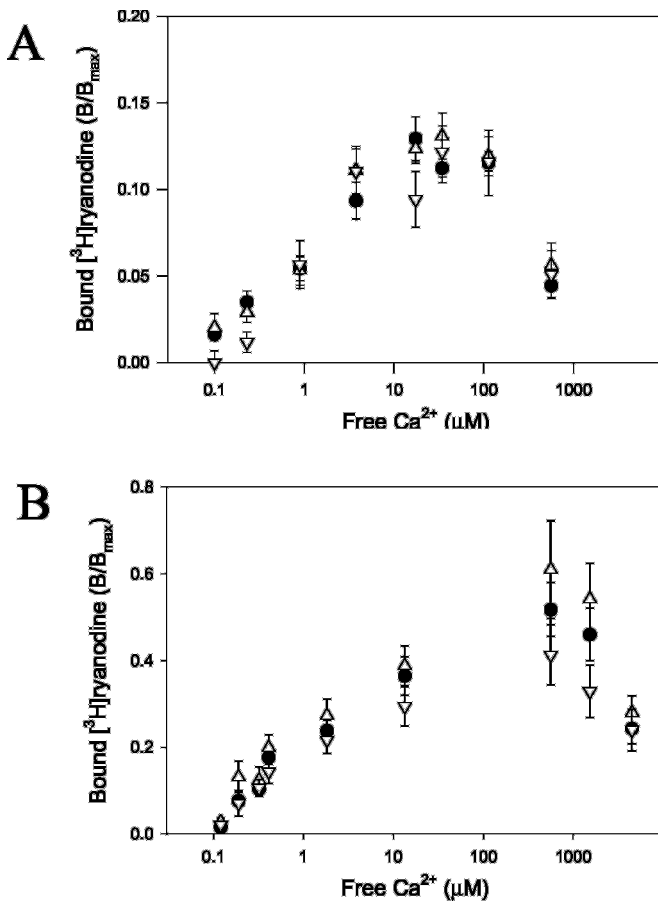


FIG. 4. Ca^{2+} dependence of skeletal and cardiac WT and mutant RyRs. *A*, skeletal WT-RyR (circles), RyR1-S2843A (triangles), and RyR1-S2843D (inverted triangles) were incubated with 2.5 nM [3 H]ryanodine in 20 mM KPipes, pH 7.0 buffer containing 0.15 M KCl, 1 mM GSSG, and the indicated free [Ca^{2+}]. *B*, corresponding experiments using cardiac WT-RyR (circles), RyR2-S2809A (triangles), and RyR2-S2809D (inverted triangles) all co-expressed with FKBP12.6. Data are mean \pm S.E. of 5–14 duplicate experiments.

tractile function during heart failure (9, 23). Following acute ischemic/reperfusion decreased RyR2 phosphorylation levels have been observed (43). In this study, we prepared two skeletal muscle and cardiac muscle RyR mutants to test the hypothesis that phosphorylation of RyR1-Ser-2843 and RyR2-Ser-2809 modifies the intrinsic channel properties of the two receptor isoforms.

RyRs are known to be regulated by a large number of exogenous and endogenous effectors and to undergo various post-translational modifications, including phosphorylation. The cy-

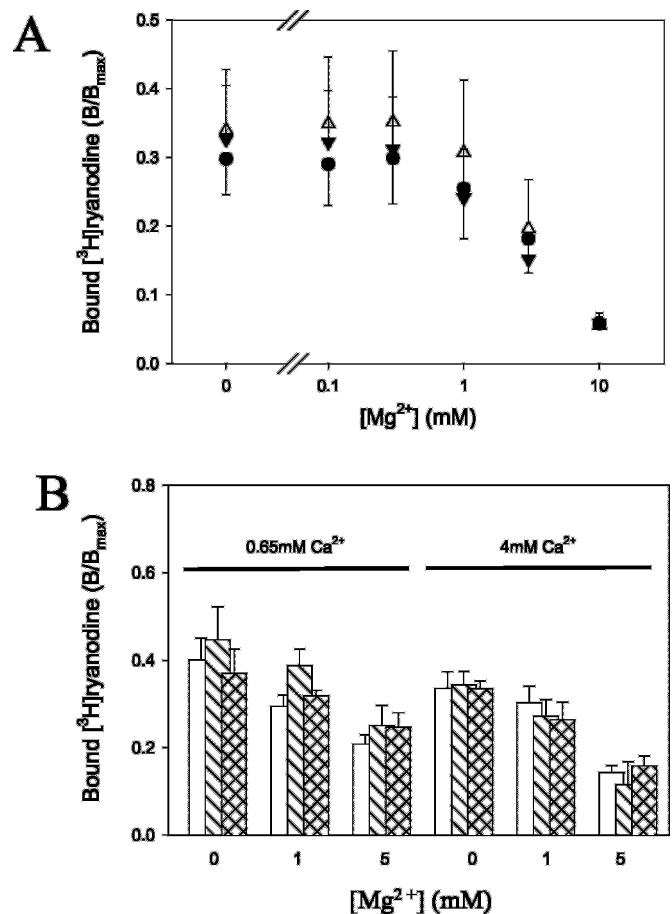


FIG. 5. Mg^{2+} dependence of cardiac WT and mutant RyR2s. *A*, membranes containing WT-RyR2 (circles), RyR2-S2809A (triangles), and RyR2-S2809D (inverted triangles) co-expressed with FKBP12.6 were incubated with 2.5 nM [3 H]ryanodine in buffer containing 0.15 M KCl, 20 mM KPipes, pH 7.0 in the presence of 1.4 mM Ca^{2+} and 1 mM GSSG. Addition of the indicated [Mg^{2+}] caused a progressive decrease in bound [3 H]ryanodine. Data are the mean \pm S.E. of 11 experiments. *B*, membranes were assayed as in *A* in the presence of 5 mM AMP-PCP and the indicated [Ca^{2+}] and [Mg^{2+}]. No significant difference between the modulation of WT-RyR2 (no lines), RyR2-S2809A (single lines), and RyR2-S2809D (crossed lines) were observed at either 0.65 mM Ca^{2+} or 4 mM free Ca^{2+} . Data are the mean \pm S.E. of 5–10 experiments.

toplasmic assembly makes up 80% of the entire channel and contains many conserved, potential phosphorylation sites. One of these sites, RyR1-Ser-2843, and the corresponding serine in the cardiac receptor, RyR2-Ser-2809, were phosphorylated by cAMP- and CaM-dependent protein kinases (12, 14). However, the presence of additional phosphorylation sites is likely as CaMKII has been shown to phosphorylate one or more three-

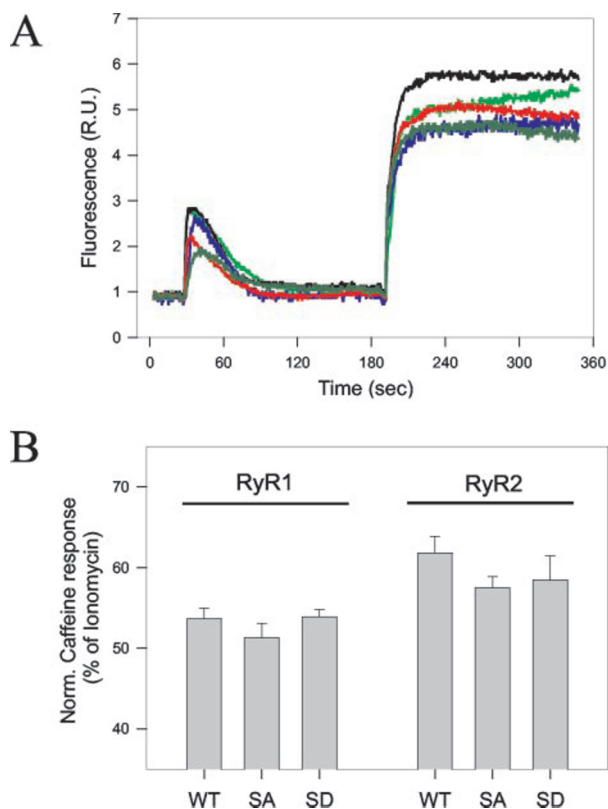


FIG. 6. Wild type and mutant RyRs exhibit similar caffeine response *in situ*. *A*, time histogram showing the response of five individual fluo-4-loaded cells expressing WT-RyR1 to 10 mM caffeine and subsequent ionomycin treatment. *B*, normalized caffeine response of WT-RyR1 (WT), RyR1-S2843A (SA), RyR1-S2843D (SD), and their cardiac equivalents co-expressed with FKBP12.6. Results are given as mean \pm S.E. of at least 15 cells from two independent experiments for WT and mutant RyRs. No significant differences were observed. R.U., response units; Norm., normalized.

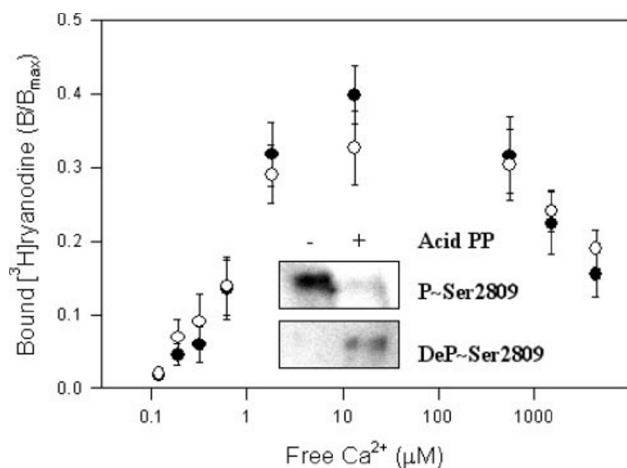


FIG. 7. Dephosphorylation of RyR2-Ser-2809 has no effect on Ca^{2+} dependence. Non-treated (filled circles) and phosphatase-treated (open circles) SR membranes were incubated with 2.5 nM [3 H]ryanodine in 20 mM KPipes, pH 7.0 buffer containing 0.15 M KCl, 1 mM GSSG, and the indicated free [Ca^{2+}]. Data are mean \pm S.E. of six duplicate experiments. The inset shows an immunoblot using anti-phospho- and anti-dephospho-RyR2-Ser-2809 antibody of 10 μ g of SR with (+) or without (-) acid phosphatase treatment. Incubation for 1 h at 37 $^{\circ}$ C caused dephosphorylation at RyR2-Ser-2809 as indicated by a decrease in phospho- and an increase in dephospho-RyR2-Ser-2809 signal. PP, protein phosphatase; P-, phospho-; DeP-, dephospho-.

nine residues in RyR (14). In support of these findings are several studies observing different functional effects for PKA- and CaMKII-phosphorylated RyRs (15, 44) and *in vitro* phos-

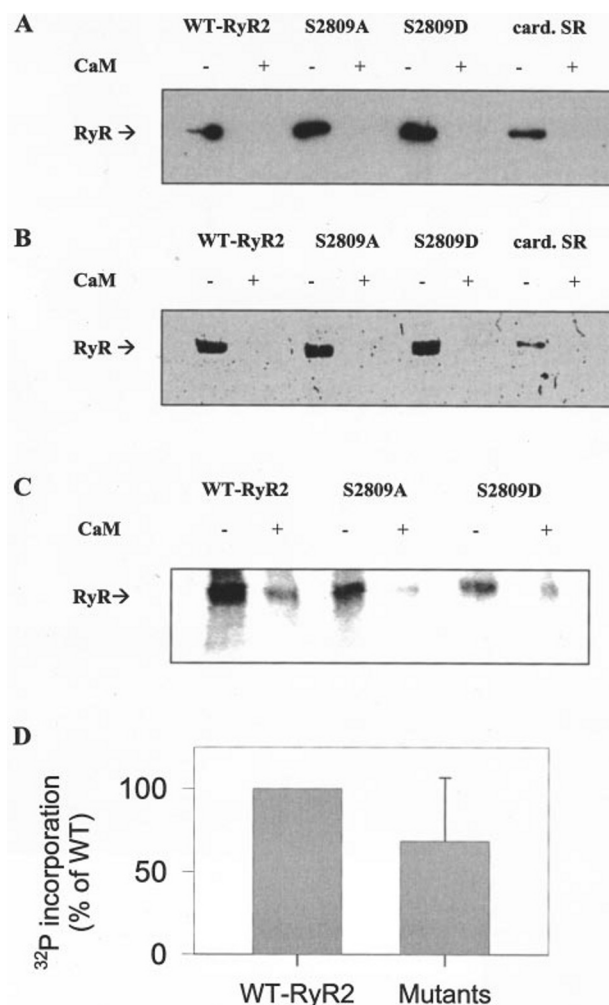


FIG. 8. RyR2 is phosphorylated at additional sites besides Ser-2809. Membrane fractions obtained from $^{32}P_i$ metabolically labeled HEK293 cells expressing cardiac WT and mutant RyR2s were solubilized in 2.5% Triton X-100 and 1 M NaCl in the presence of protein phosphatase inhibitors and purified using CaM-agarose beads. *A*, representative Western blot showing CaM batch-purified unlabeled WT-RyR2, RyR2-S2809A, and RyR2-S2809D in the presence and absence of 3 μ M CaM. *B*, silver-stained gels of parallel processed ^{32}P -labeled samples. The identified position of RyR2 in Western blots correlated with a single high molecular weight band observed in silver-stained gels. *C*, representative autoradiogram depicting levels of ^{32}P incorporation in WT-RyR2, RyR2-S2809A, and RyR2-S2809D protein bands. *D*, normalized RyR2 ^{32}P incorporation of mutant receptors relative to WT-RyR2. Results are mean \pm S.E. of two experiments combining data obtained with RyR2-S2809A and RyR2-S2809D. card., cardiac.

phorylation assays using phosphorylation state-dependent antibodies that have suggested the presence of at least four CaMK phosphorylation sites in addition to RyR2-Ser-2809 (16). Our finding that the two RyR2-Ser-2809 mutants with a serine to alanine or aspartic acid substitution incorporate $^{32}P_i$ in metabolic labeling experiments confirms the earlier findings and indicates that the receptor may be phosphorylated *in vivo* at more than one site. *In vitro* phosphorylation studies have also indicated that protein kinase C and protein kinase G phosphorylate RyR1 (14); however, regulation of the receptor by these kinases under physiological conditions remains to be established.

RyR1 and RyR2 are part of a multiprotein complex that includes the tightly associated FK506-binding proteins (9, 23). FK506 and rapamycin released FKBP12 from the RyR1 complex and FKBP12.6 from the RyR2 complex and modulated channel gating by increasing channel activity and inducing

frequent subconductances in lipid bilayers (Ref. 45 but see also Ref. 46). PKA-mediated RyR phosphorylation has been reported to also be associated with the release of the FKBP from the RyR protein complexes and increased channel activities in lipid bilayers. Moreover, Marks and colleagues (9, 23) found that RyR1 from skeletal muscle and RyR2 from hearts of animal models of heart failure and human failing hearts are hyperphosphorylated, are depleted of the FKBP, and exhibit increased channel activities. These findings led them to propose that hyperphosphorylated RyRs are leaky and therefore lead to a reduced SR Ca^{2+} load and impaired contractile function in heart failure. Marks and colleagues also characterized three recombinant RyR phosphorylation mutants (RyR1-S2843A, RyR1-S2843D, and RyR2-S2809D) following transient expression in HEK293 cells (23, 47). The RyR1-S2843A mutant in lipid bilayer measurements exhibited a single channel behavior similar to WT-RyR1 as observed in the present study. However, different results were obtained with the recombinant RyR1-S2843D and RyR2-S2809D mutants with the RyR2-S2809D mutants showing a more than 2-fold increase in open probability compared with WT receptor and the RyR1-S2843D mutation causing an ~ 100 -fold increase in channel activity. The recordings showed an increase in the number of channel events, and current histograms indicated the appearances of substates similar to those observed in native, PKA-phosphorylated RyR.

In this study, we found that in single channel measurements P_o values, frequency of full open events and substates, and mean open and closed times were not significantly different for WT and mutants for both the skeletal and cardiac RyR isoforms. We also analyzed Ca^{2+} -mediated activation and inactivation of WT and mutant receptors in [^3H]ryanodine binding experiments as well as the caffeine response of transiently expressed WT and mutant receptors in calcium imaging experiments. In both assays, we were unable to detect an increased activity of the RyR1-S2843D or RyR2-S2809D mutants over that of WT. Marks and colleagues (23, 47) used co-immunoprecipitation experiments to also show that RyR1-S2843D and RyR2-S2809D lost their ability to bind FKBP12. Loss of this accessory protein in the mutant and hyperphosphorylated native RyRs was suggested to account for the observed changes in channel gating. Indeed rebinding of a "sticky" FKBP12.6-D37S mutant that was able to bind to the phosphorylated RyR2 restored normal RyR2-S2809D channel function. Our co-immunoprecipitation data showed that RyR1-S2843D and RyR2-S2809D bind the FKBP to an extent similar to WT, RyR1-S2843A, and RyR2-S2809A receptors. Differences in the experimental conditions may account for the differences in FKBP binding observed by Marks and colleagues and the present study. To ensure that the immunoprecipitated FKBP did not bind to other proteins present in the membrane fractions, we performed co-immunoprecipitation experiments with $100,000 \times g$ supernatant fractions. High salt (1 M NaCl) and detergent (2.5% Triton X-100) concentrations were required to solubilize WT and mutant receptors. RyR solubilization for 12 h at 4 °C in modified radioimmune precipitation assay buffer and low salt concentrations (154 mM NaCl), conditions used by Reiken *et al.* (23) for skeletal and by Marx *et al.* (9) for cardiac RyR, resulted in an only small extent of RyR solubilization in our experiments.

Back-phosphorylation (48) and the use of phosphorylation state-dependent antibodies (Ref. 16 and this study) indicate that cardiac SR exhibits substantial endogenous phosphorylation levels at RyR2-Ser-2809. Treatment of cardiac SR with acid phosphatase (Fig. 7) and alkaline phosphatase (data not shown) caused dephosphorylation of RyR2-Ser-2809 without

affecting RyR2 activity in [^3H]ryanodine binding experiments. This observation is in agreement with the finding of a similar regulation of our mutants, which mimic the phosphorylated and dephosphorylated receptors.

In conclusion, in this study we tested the hypothesis of Marks and colleagues (9, 23) that PKA-mediated hyperphosphorylation of a conserved serine, Ser-2843 in skeletal RyR and Ser-2809 in cardiac RyR, results in an aberrant SR function during heart failure. We found that substitution of Ser-2809 in RyR2 and Ser-2843 in RyR1 with an aspartic acid neither resulted in the release of the associated FK506-binding proteins nor modified the intrinsic channel properties of the two receptor isoforms. Further studies are necessary that are beyond the scope of this work to clarify the role of protein phosphorylation on RyR2 function in normal and failing hearts. These include the possibility that phosphorylation of the RyRs at additional sites may alter intrinsic RyR function as well as affect the binding of RyR accessory proteins such as the FKBP.

Acknowledgment—We thank Daniel A. Pasek for preparing the cardiac and skeletal muscle membrane fractions.

REFERENCES

- Rios, E., and Pizarro, G. (1991) *Physiol. Rev.* **71**, 849–908
- Fabiato, A. (1983) *Am. J. Physiol.* **245**, C1–C14
- Franzini-Armstrong, C., Protasi, F., and Ramesh, V. (1999) *Biophys. J.* **77**, 1528–1539
- Franzini-Armstrong, C., and Protasi, F. (1997) *Physiol. Rev.* **77**, 699–729
- Fill, M., and Copello, J. A. (2002) *Physiol. Rev.* **82**, 893–922
- Brillantes, A. B., Ondrias, K., Scott, A., Koblinsky, E., Ondriasova, E., Moschella, M. C., Jayaraman, T., Landers, M., Ehrlich, B. E., and Marks, A. R. (1994) *Cell* **77**, 513–523
- Marx, S. O., Ondrias, K., and Marks, A. R. (1998) *Science* **281**, 818–821
- Marx, S. O., Gaburjakova, J., Gaburjakova, M., Henrikson, C., Ondrias, K., and Marks, A. R. (2001) *Circ. Res.* **88**, 1151–1158
- Marx, S. O., Reiken, S., Hisamatsu, Y., Jayaraman, T., Burkoff, D., Rosemblyt, N., and Marks, A. R. (2000) *Cell* **101**, 365–376
- Bandyopadhyay, A., Shin, D. W., Ahn, J. O., and Kim, D. H. (2000) *Biochem. J.* **352**, 61–70
- Meissner, G. (2002) *Front. Biosci.* **7**, d2072–d2080
- Witcher, D. R., Kovacs, R. J., Schulman, H., Cefali, D. C., and Jones, L. R. (1991) *J. Biol. Chem.* **266**, 11144–11152
- Chu, A., Sumbilla, C., Inesi, G., Jay, S. D., and Campbell, K. P. (1990) *Biochemistry* **29**, 5899–5905
- Suko, J., Maurer, F. I., Plank, B., Wiskovsky, W., Hohenegger, M., and Hellmann, G. (1993) *Biochim. Biophys. Acta* **1175**, 193–206
- Hain, J., Onoue, H., Mayrleitner, M., Fleischer, S., and Schindler, H. (1995) *J. Biol. Chem.* **270**, 2074–2081
- Rodriguez, P., Bhogal, M. S., and Colyer, J. (2003) *J. Biol. Chem.* **278**, 38593–38600
- Hohenegger, M., and Suko, J. (1993) *Biochem. J.* **296**, 303–308
- Dulhunty, A. F., Laver, D., Curtis, S. M., Pace, S., Haarmann, C., and Gallant, E. M. (2001) *Biophys. J.* **81**, 3240–3252
- Bayer, K. U., Harbers, K., and Schulman, H. (1998) *EMBO J.* **17**, 5598–5605
- Uehara, A., Yasukochi, M., Mejia-Alvarez, R., Fill, M., and Imanaga, I. (2002) *Pflueg. Arch. Eur. J. Physiol.* **444**, 202–212
- Valdivia, H. H., Kaplan, J. H., Ellis-Davies, G. C., and Lederer, W. J. (1995) *Science* **267**, 1997–2000
- Ward, C. W., Reiken, S., Marks, A. R., Marty, I., Vassort, G., and Lacampagne, A. (2003) *FASEB J.* **17**, 1517–1519
- Reiken, S., Lacampagne, A., Zhou, H., Kherani, A., Lehnart, S. E., Ward, C., Huang, F., Gaburjakova, M., Gaburjakova, J., Rosemblyt, N., Warren, M. S., He, K. L., Yi, G. H., Wang, J., Burkoff, D., Vassort, G., and Marks, A. R. (2003) *J. Cell Biol.* **160**, 919–928
- Yano, M., Ono, K., Ohkusa, T., Suetsugu, M., Kohno, M., Hisaoka, T., Kobayashi, S., Hisamatsu, Y., Yamamoto, T., Noguchi, N., Takasawa, S., Okamoto, H., and Matsuzaki, M. (2000) *Circulation* **102**, 2131–2136
- Jiang, M. T., Lokuta, A. J., Farrell, E. F., Wolff, M. R., Haworth, R. A., and Valdivia, H. H. (2002) *Circ. Res.* **91**, 1015–1022
- Li, Y., Kranias, E. G., Mignery, G. A., and Bers, D. M. (2002) *Circ. Res.* **90**, 309–316
- Gao, L., Tripathy, A., Lu, X., and Meissner, G. (1997) *FEBS Lett.* **412**, 223–226
- Nakai, J., Imagawa, T., Hakamata, Y., Shigekawa, M., Takeshima, H., and Numa, S. (1990) *FEBS Lett.* **271**, 169–177
- Meissner, G. (1984) *J. Biol. Chem.* **259**, 2365–2374
- Meissner, G., and Henderson, J. S. (1987) *J. Biol. Chem.* **262**, 3065–3073
- Stange, M., Tripathy, A., and Meissner, G. (2001) *Biophys. J.* **81**, 1419–1429
- Sutko, J. L., Airey, J. A., Welch, W., and Ruest, L. (1997) *Pharmacol. Rev.* **49**, 53–98
- Balshaw, D. M., Xu, L., Yamaguchi, N., Pasek, D. A., and Meissner, G. (2001) *J. Biol. Chem.* **276**, 20144–20153
- Fessenden, J. D., Wang, Y., Moore, R. A., Chen, S. R., Allen, P. D., and Pessah, I. N. (2000) *Biophys. J.* **79**, 2509–2525
- Schoenmakers, T. J., Visser, G. J., Flick, G., and Theuvenet, A. P. (1992)

- BioTechniques* **12**, 870–879
36. Hain, J., Nath, S., Mayrleitner, M., Fleischer, S., and Schindler, H. (1994) *Biophys. J.* **67**, 1823–1833
37. Szegedi, C., Sarkozi, S., Herzog, A., Jona, I., and Varsanyi, M. (1999) *Biochem. J.* **337**, 19–22
38. Narayanan, N., and Xu, A. (1997) *Basic Res. Cardiol.* **92**, 25–35
39. Simmerman, H. K., and Jones, L. R. (1998) *Physiol. Rev.* **78**, 921–947
40. Guo, W., Jorgensen, A. O., and Campbell, K. P. (1994) *J. Biol. Chem.* **269**, 28359–28365
41. Damiani, E., Picello, E., Saggin, L., and Margreth, A. (1995) *Biochem. Biophys. Res. Commun.* **209**, 457–465
42. Lokuta, A. J., Meyers, M. B., Sander, P. R., Fishman, G. I., and Valdivia, H. H. (1997) *J. Biol. Chem.* **272**, 25333–25338
43. Temsah, R. M., Dyck, C., Neticadan, T., Chapman, D., Elimban, V., and Dhalla, N. S. (2000) *J. Pharmacol. Exp. Ther.* **293**, 15–23
44. Lokuta, A. J., Rogers, T. B., Lederer, W. J., and Valdivia, H. H. (1995) *J. Physiol.* **487**, 609–622
45. Gaburjakova, M., Gaburjakova, J., Reiken, S., Huang, F., Marx, S. O., Rosemblyt, N., and Marks, A. R. (2001) *J. Biol. Chem.* **276**, 16931–16935
46. Timerman, A. P., Onoue, H., Xin, H. B., Barg, S., Copello, J., Wiederrecht, G., and Fleischer, S. (1996) *J. Biol. Chem.* **271**, 20385–20391
47. Wehrens, X. H., Lehnart, S. E., Huang, F., Vest, J. A., Reiken, S. R., Mohler, P. J., Sun, J., Guatimosim, S., Song, L. S., Rosemblyt, N., D'Armiento, J. M., Napolitano, C., Memmi, M., Priori, S. G., Lederer, W. J., and Marks, A. R. (2003) *Cell* **113**, 829–840
48. Zhang, T., Maier, L. S., Dalton, N. D., Miyamoto, S., Ross, J., Jr., Bers, D. M., and Brown, J. H. (2003) *Circ. Res.* **92**, 912–919